Correlators Exceeding One in Continuous Measurements of Superconducting Qubits

Juan Atalaya,[1,*] Shay Hacohen-Gourgy,[2,3,4] Irfan Siddiqi,[2,3] and Alexander N. Korotkov[1,†]
[1]Department of Electrical and Computer Engineering, University of California, Riverside, California 92521, USA
[2]Quantum Nanoelectronics Laboratory, Department of Physics, University of California, Berkeley, California 94720, USA
[3]Center for Quantum Coherent Science, University of California, Berkeley, California 94720, USA
[4]Department of Physics, Technion, Haifa 3200003, Israel

(Received 12 September 2018; published 7 June 2019)

We consider the effect of phase backaction on the correlator $\langle I(t)I(t+\tau)\rangle$ for the output signal $I(t)$ from continuous measurement of a qubit. We demonstrate that the interplay between informational and phase backactions in the presence of Rabi oscillations can lead to the correlator becoming larger than 1, even though $|\langle I\rangle| \leq 1$. The correlators can be calculated using the generalized "collapse recipe," which we validate using the quantum Bayesian formalism. The recipe can be further generalized to the case of multitime correlators and arbitrary number of detectors, measuring non-commuting qubit observables. The theory agrees well with experimental results for continuous measurement of a transmon qubit. The experimental correlator exceeds the bound of 1 for a sufficiently large angle between the amplified and informational quadratures, causing the phase backaction. The demonstrated effect can be used to calibrate the quadrature misalignment.

DOI: 10.1103/PhysRevLett.122.223603

Introduction.—Continuous quantum measurements (CQMs) are attracting significant attention in quantum computing and quantum physics. Although they have been theoretically discussed for a long time using various approaches [1–9], current interest in CQMs is mainly motivated by relatively recent experiments with superconducting qubits [10–16]. They are useful for quantum computing applications such as quantum feedback [17–21], rapid state purification [22], preparation of entangled states [14,23,24], and continuous quantum error correction [25,26]. CQMs are also shedding light on our understanding of the still debatable quantum measurement process, including nontrivial cases such as simultaneous CQM of noncommuting observables [15,16,27].

Temporal correlators of the output signals from CQMs are important objects to study because they bear nonclassical features due to the interplay between coherent quantum evolution and measurement-induced quantum backaction. In particular, violation of a classical bound is a clear indication of quantum behavior. As an example, macrorealism assumptions have been tested with correlators from CQM via the continuous Leggett-Garg inequality [11]. There is significant recent interest in correlators from CQMs [28–33], including multitime correlators and the case of noncommuting observables. In particular, multitime correlators are important in the continuous operation of quantum subsystem codes [34].

Quantum backaction from measurement can be described in terms of Kraus operators [1]. The polar decomposition of a Kraus operator suggests, in general, two types of quantum backaction that are related to the nonunitary and unitary factors of the polar decomposition. In particular, in circuit QED-based measurements of superconducting qubits they are often referred to as informational backaction and phase backaction, respectively [9,13,35]. Circuit QED systems are ideal to study these two types of quantum backaction because their relative strength is easily tunable by the phase of the pump applied to a phase-sensitive parametric amplifier [8,9,13].

In this Letter, we study the effect of phase backaction on output-signal correlators for continuous measurement of a superconducting qubit. We present a general theory for multitime correlators in the spirit of the "collapse recipe" [30,32,36], which is extended here to include phase backaction and proven using the quantum Bayesian formalism. In such a generalized recipe, correlators from continuous qubit measurements can be calculated by assuming fictitious "strong" measurements (with discrete outcomes ± 1) at the time moments entering the correlator and assuming ensemble-averaged evolution at other times. Importantly, the fictitious strong measurements can move the qubit state *outside the Bloch sphere*, and correspondingly the outcome probabilities for the next strong measurement can be negative. Even though the procedure is bizarre from a physical point of view, this is a simple way to obtain correct correlators, including the case of simultaneous CQM of noncommuting qubit observables and arbitrary coherent evolution and decoherence.

In particular, our theory predicts the counterintuitive result that *correlators can be larger than* 1, even though the average value of the output is between ± 1. To test this prediction, we perform CQM of σ_z (Fig. 1) and show that

 © 2019 American Physical Society

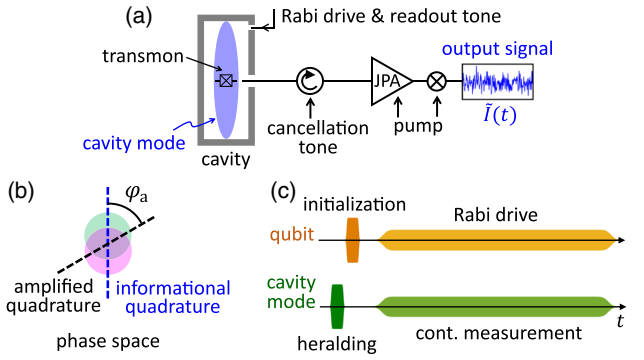

FIG. 1. (a) Schematic illustration of the experimental setup for continuous measurement of qubit observable σ_z. A superconducting qubit is dispersively coupled to a 3D microwave resonator. The leaked field is amplified by a phase-sensitive Josephson parametric amplifier (JPA), producing the (downconverted) normalized output signal $I(t)$. The cancellation tone displaces the outgoing field close to the vacuum, thus preventing JPA saturation. The coherent states corresponding to the eigenstates of σ_z are illustrated in panel (b) by two circles in phase space. The line through their centers defines the informational quadrature, while the JPA's pump phase defines the amplified quadrature. The angle φ_a between them affects the phase backaction. (c) Experimental pulse sequence.

the experimental correlators indeed exceed unity when we use a sufficiently strong phase backaction and sufficiently fast Rabi oscillations. Note that such nonclassical values would be natural for weak values [37]; however, our experiment is not related to weak values since it does not use postselection.

The quantum Bayesian formalism.—As the simplest case, let us consider a Rabi-rotated qubit under continuous σ_z measurement in the typical circuit QED setup with a phase-sensitive amplifier [13,15]—see Fig. 1. In this case the relative strength of the phase backaction and informational backaction is controlled by the angle φ_a between the amplified and informational quadratures [8,9]. We will discuss the correlator ($t_2 > t_1$)

$$K(t_1, t_2) \equiv \langle I(t_2) I(t_1) \rangle, \tag{1}$$

where $I(t) = [\tilde{I}(t) - \tilde{I}_o]/\Delta I(\varphi_a)$ is the normalized output signal, $\tilde{I}(t)$ is the actual experimental output, $\tilde{I}_o$ is the offset, and $\Delta I(\varphi_a) = \Delta I_{\max} \cos\varphi_a$ is the response, so that this normalization provides $\langle I \rangle = 1$ or -1 when the qubit is in the state $|1\rangle$ or $|0\rangle$, respectively (the symbol $\langle .. \rangle$ means ensemble average). The normalized signal can be modeled as [7,32]

$$I(t) = \mathrm{Tr}[\sigma_z \rho(t)] + \sqrt{\tau_m}\xi(t) = \boldsymbol{z}\boldsymbol{r}(t) + \sqrt{\tau_m}\xi(t), \tag{2}$$

where $\boldsymbol{r} = (x, y, z)$ is the Bloch vector defined by the qubit density matrix parametrization $\rho = (\mathbb{1} + x\sigma_x + y\sigma_y + z\sigma_z)/2$ and $\boldsymbol{z} = (0, 0, 1)$ is the measurement axis direction corresponding to the measured observable $\sigma_z = |1\rangle\langle 1| - |0\rangle\langle 0|$. The white Gaussian noise $\xi(t)$ has zero average, $\langle \xi(t) \rangle = 0$, and two-time correlator

$$\langle \xi(t)\xi(t') \rangle = \delta(t - t'). \tag{3}$$

The "measurement time" $\tau_m = \tau_{\min}/\cos^2\varphi_a$ in Eq. (2) is the time to reach the signal-to-noise ratio of 1.

The qubit evolution can be described by the quantum Bayesian equation [8,9] (in Itô interpretation)

$$\dot{\boldsymbol{r}} = \Lambda_{\mathrm{ens}}(\boldsymbol{r} - \boldsymbol{r}_{\mathrm{st}}) + \frac{\boldsymbol{z} - (\boldsymbol{z}\boldsymbol{r})\boldsymbol{r}}{\sqrt{\tau_m}}\xi(t) + \mathcal{K}\frac{\boldsymbol{z} \times \boldsymbol{r}}{\sqrt{\tau_m}}\xi(t), \tag{4}$$

where the first term is the ensemble-averaged evolution, the second term is the informational backaction, and the third term is the phase backaction with $\mathcal{K} = \tan\varphi_a$. The evolution of the ensemble-averaged state $\boldsymbol{r}_{\mathrm{ens}} \equiv \langle \boldsymbol{r} \rangle$,

$$\dot{\boldsymbol{r}}_{\mathrm{ens}} = \Lambda_{\mathrm{ens}}(\boldsymbol{r}_{\mathrm{ens}} - \boldsymbol{r}_{\mathrm{st}}), \tag{5}$$

is characterized by the 3×3 matrix Λ_{ens} and stationary state $\boldsymbol{r}_{\mathrm{st}}$; this evolution corresponds to the Lindblad-form equation, $\dot{\rho}_{\mathrm{ens}} = -(i/\hbar)[H_q, \rho_{\mathrm{ens}}] + \mathcal{L}[\rho_{\mathrm{ens}}]$, where H_q is the qubit Hamiltonian and $\mathcal{L}$ describes the qubit ensemble decoherence. In our case, the contribution to $\mathcal{L}$ due to measurement is $\mathcal{L}_m[\rho] = \Gamma_m[\sigma_z \rho \sigma_z - \rho]/2$, where $\Gamma_m = (1 + \mathcal{K}^2)/(2\eta\tau_m) = 1/(2\eta\tau_{\min})$ is the measurement-induced ensemble dephasing rate and η is the detector quantum efficiency. Note that Γ_m does not depend on φ_a, in contrast to $\mathcal{K}$ and τ_m.

Collapse recipe.—The collapse recipe was previously introduced to calculate two-time correlators [36] and multitime correlators [32] without phase backaction. For the correlator (1), this recipe states that we should replace continuous measurement at time moments t_1 and t_2 by (fictitious) projective measurements and use ensemble-averaged evolution at any other time. The projective measurements probabilistically produce discrete results $I_k = \pm 1$ and correspondingly collapse the qubit to $|1\rangle$ or $|0\rangle$.

As proven below, in the presence of phase backaction, the correlator (1) still can be calculated in a somewhat similar way; however, we should use a quite unusual generalized collapse recipe (GCR). In particular, after a projective measurement at time t_1 with the result $I_1 = \pm 1$, the qubit state collapses to $I_1 \boldsymbol{r}_{\mathrm{coll}}$, where

$$\boldsymbol{r}_{\mathrm{coll}} = \boldsymbol{z} + \mathcal{K}(\boldsymbol{z} \times \boldsymbol{r}_1) \tag{6}$$

and $\boldsymbol{r}_1 \equiv \boldsymbol{r}(t_1 - 0)$ is the qubit state just before the collapse. We emphasize that, excluding the case when $\boldsymbol{z} \times \boldsymbol{r}_1 = \boldsymbol{0}$ or $\mathcal{K} = 0$, state (6) is outside the Bloch sphere. After the collapse at time t_1, the qubit evolves according to Eq. (5). Thus, using the GCR, the correlator (1) can be calculated as

$$K(t_1,t_2)=\sum_{I_1,I_2=\pm1} I_1 I_2 p(I_2,t_2|I_1,t_1)p(I_1,t_1), \quad (7)$$

where the sum is over four scenarios of outcomes,

$$p(I_1,t_1)=\frac{1+I_1 z r_1}{2} \quad (8)$$

is the probability to get the first outcome $I_1=\pm1$, and

$$p(I_2,t_2|I_1,t_1)=\frac{1+I_2 z r_{\rm ens}(t_2|I_1 r_{\rm coll},t_1)}{2}, \quad (9)$$

is the "conditional probability" to get the outcome $I_2=\pm1$ at time t_2 given that we got outcome I_1 at time t_1. Here $r_{\rm ens}(t|r_{\rm in},t_{\rm in})$ denotes the solution of Eq. (5) with initial condition $r_{\rm ens}(t_{\rm in})=r_{\rm in}$ at time $t_{\rm in}<t$. Since $r_{\rm ens}$ can be outside the Bloch sphere, the "probability" (9) can be negative or larger than 1; however, the normalization condition $\sum_{I_2=\pm1} p(I_2,t_2|I_1,t_1)=1$ still holds. If the qubit is prepared in a state r_0 ($|r_0|\le 1$) at $t_0<t_1$, then $r_1=r_{\rm ens}(t_1|r_0,t_0)$ is within the Bloch sphere, so the first probability (8) has the usual range of values. Note that the recipe for multitime correlators (discussed below) has essentially the same form.

GCR from the quantum Bayesian formalism.—Let us prove the recipe of Eqs. (6)–(9) using Eqs. (2)–(5). The proof somewhat follows Refs. [30,32]. First, we rewrite Eq. (7) of the GCR as

$$K(t_1,t_2)=z[r_{\rm ens}(t_2|r_{\rm coll},t_1)(1+z_1)/2 - r_{\rm ens}(t_2|-r_{\rm coll},t_1)(1-z_1)/2], \quad (10)$$

where $z_1\equiv z r_1$ and $t_2>t_1$. Next, we calculate the correlator (1) directly and show that the result coincides with Eq. (10). Using Eq. (2), we decompose the correlator as

$$K(t_1,t_2)=z[\boldsymbol{K}^{(1)}(t_1,t_2)+\boldsymbol{K}^{(2)}(t_1,t_2)], \quad (11)$$

where the vector-valued correlators $\boldsymbol{K}^{(1,2)}$ are defined as

$$\boldsymbol{K}^{(1)}(t_1,t_2)\equiv\langle \boldsymbol{r}(t_2)\rangle z_1,$$
$$\boldsymbol{K}^{(2)}(t_1,t_2)\equiv\langle \boldsymbol{r}(t_2)\sqrt{\tau_m}\xi(t_1)\rangle. \quad (12)$$

Differentiating $\boldsymbol{K}^{(1)}$ over t_2 and using Eq. (4), we find that $\boldsymbol{K}^{(1)}$ satisfies an equation similar to Eq. (5),

$$\partial_{t_2}\boldsymbol{K}^{(1)}(t_1,t_2)=\Lambda_{\rm ens}[\boldsymbol{K}^{(1)}(t_1,t_2)-z_1 r_{\rm st}], \quad (13)$$

with initial condition $\boldsymbol{K}^{(1)}(t_1,t_1)=r_1 z_1$. Therefore,

$$\boldsymbol{K}^{(1)}(t_1,t_2)=\mathcal{P}(t_2|t_1)z_1 r_1+z_1\boldsymbol{\mathcal{P}}_{\rm st}(t_2|t_1), \quad (14)$$

where $\mathcal{P}(t|t')$ is a 3×3 matrix satisfying equation $\partial_t\mathcal{P}(t|t')=\Lambda_{\rm ens}(t)\mathcal{P}(t|t')$ with $\mathcal{P}(t'|t')=\mathbb{1}$, and $\boldsymbol{\mathcal{P}}_{\rm st}(t|t')=-\int_{t'}^{t}\mathcal{P}(t|t'')\Lambda_{\rm ens}(t'')r_{\rm st}(t'')dt''$ is a vector.

Similarly, $\boldsymbol{K}^{(2)}$ satisfies equation

$$\partial_{t_2}\boldsymbol{K}^{(2)}(t_1,t_2)=\Lambda_{\rm ens}\boldsymbol{K}^{(2)}(t_1,t_2), \quad (15)$$

in which there is no term proportional to $r_{\rm st}$, in contrast to Eq. (13), because $\langle\Lambda_{\rm ens}r_{\rm st}\xi(t)\rangle=0$. To find the initial condition $\boldsymbol{K}^{(2)}(t_1,t_1+0)$, we discretize Eq. (4) with a timestep δt and obtain $r(t_1+\delta t)-r(t_1)\approx[z-z_1 r_1+\mathcal{K}(z\times r_1)]\delta t\xi(t_1)/\sqrt{\tau_m}$, which has a typical size $\sim\sqrt{\delta t}$ since $\langle\xi^2(t_1)\rangle=(\delta t)^{-1}$—see Eq. (3). Inserting this result for $r(t_1+\delta t)$ into Eq. (12), we obtain $\boldsymbol{K}^{(2)}(t_1,t_1+0)=z-z_1 r_1+\mathcal{K}(z\times r_1)$ in the limit $\delta t\to0$. Thus,

$$\boldsymbol{K}^{(2)}(t_1,t_2)=\mathcal{P}(t_2|t_1)[r_{\rm coll}-z_1 r_1], \quad (16)$$

so that τ_m in the definition (12) of $\boldsymbol{K}^{(2)}$ cancels out.

From Eqs. (11), (14), and (16), we obtain

$$K(t_1,t_2)=z[\mathcal{P}(t_2|t_1)r_{\rm coll}+z_1\boldsymbol{\mathcal{P}}_{\rm st}(t_2|t_1)], \quad (17)$$

with the terms proportional to $z_1 r_1$ in Eqs. (14) and (16) exactly canceling each other and not contributing to Eq. (17). This is expected from linearity of quantum mechanics, which requires a linear (not quadratic) dependence of the correlators on the initial state.

Finally, formally solving Eq. (5) as $r_{\rm ens}(t|r_{\rm in},t_{\rm in})=\mathcal{P}(t|t_{\rm in})r_{\rm in}+\boldsymbol{\mathcal{P}}_{\rm st}(t|t_{\rm in})$ and using this solution in Eq. (10), we see that the result exactly coincides with Eq. (17). This proves that the GCR yields the same correlator as the one obtained from the quantum Bayesian formalism.

We emphasize that even though the GCR is quite useful for calculation of correlators, actual quantum trajectories are described by the much more complicated quantum Bayesian equation (4). In particular, quantum state tomography would not find the qubit state outside the Bloch sphere. Nevertheless, since the GCR leads to correct correlators, it can give us an intuition for predicting correlators from continuous measurements.

Experimental correlators larger than 1.—Next we discuss that the effective qubit evolution outside the Bloch sphere leads to correlators larger than 1 in the experiment illustrated in Fig. 1. In the experiment the qubit undergoes Rabi oscillations with frequency Ω_R over the x axis and continuous measurement of σ_z. Neglecting energy relaxation, the ensemble-averaged evolution is described by Eq. (5) with $r_{\rm st}=0$ (i.e., unital evolution) and

$$\Lambda_{\rm ens}=\begin{pmatrix}-\Gamma & 0 & 0\\ 0 & -\Gamma & -\Omega_R\\ 0 & \Omega_R & 0\end{pmatrix}, \quad (18)$$

where Γ is the ensemble dephasing rate, which is mostly due to measurement, $\Gamma \approx \Gamma_m$. Because of unitality ($\boldsymbol{r}_{\rm st} = 0$), there is a symmetry

$$\boldsymbol{r}_{\rm ens}(t|-\boldsymbol{r}_{\rm in}, t_{\rm in}) = -\boldsymbol{r}_{\rm ens}(t|\boldsymbol{r}_{\rm in}, t_{\rm in}), \tag{19}$$

so Eq. (10) for the correlator reduces to only one term,

$$K(t_1, t_2) = \boldsymbol{z}\boldsymbol{r}_{\rm ens}(t_2|\boldsymbol{r}_{\rm coll}, t_1), \tag{20}$$

and therefore in the GCR we can pretend that the measurement result at t_1 is always $I_1 = +1$. This moves the qubit to the state $\boldsymbol{r}_{\rm coll}$ given by Eq. (6), and the correlator is simply the qubit z component at time t_2, i.e., $K = z_{\rm ens} \equiv \boldsymbol{z}\boldsymbol{r}_{\rm ens}$.

In the experiment, the qubit is prepared at time $t_0 = 0$ in the state $\boldsymbol{r}_0 = (x_0, 0, 0)$ with $x_0 = \pm 1$ (i.e., along the rotation axis). Without the intuition provided by the GCR, this choice to observe correlators larger than 1 is counterintuitive. However, according to the GCR, the effective after-collapse qubit evolution starts outside the Bloch sphere at the state

$$\boldsymbol{r}_{\rm coll} = (0, x_1 \tan\varphi_a, 1), \qquad x_1 = x_0 \exp(-\Gamma t_1), \tag{21}$$

which after Rabi rotation can have z component up to $\sqrt{1 + x_1^2 \tan^2\varphi_a}$. This geometrical picture is illustrated in Fig. 2, making clear that both phase backaction and Rabi oscillations are necessary to observe $K > 1$.

In the experiment, the correlator is additionally time averaged in order to reduce fluctuations,

$$K(\tau) \equiv \frac{1}{T}\int_{t_{\rm skip}}^{t_{\rm skip}+T} K(t_1, t_1+\tau)dt_1, \tag{22}$$

where T is the averaging duration, which starts with a small delay $t_{\rm skip}$ to skip initial transients. Using the GCR, we obtain—see the Supplemental Material [38],

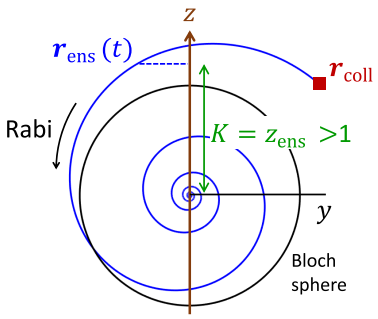

FIG. 2. Qubit evolution in the GCR picture. At time t_1, the qubit state jumps to $\boldsymbol{r}_{\rm coll}$ [Eq. (21)], which is outside the Bloch sphere when phase backaction is present. Rabi oscillations then can produce z component $z_{\rm ens} \equiv \boldsymbol{z}\boldsymbol{r}_{\rm ens}$ larger than 1, so that the correlator $K(t_1, t_2) = z_{\rm ens}(t_2)$ exceeds 1.

$$K(\tau) = \left(\cos(\tilde{\Omega}_R\tau) + \frac{\Gamma}{2\tilde{\Omega}_R}\sin(\tilde{\Omega}_R\tau)\right)e^{-\Gamma\tau/2} + \tan\varphi_a \frac{cx_0\Omega_R}{\tilde{\Omega}_R}\sin(\tilde{\Omega}_R\tau)e^{-\Gamma\tau/2}, \tag{23}$$

where $c = \exp(-\Gamma t_{\rm skip})[1 - \exp(-\Gamma T)]/(\Gamma T)$ and $\tilde{\Omega}_R \equiv \sqrt{\Omega_R^2 - \Gamma^2/4}$. This correlator does not depend on the quantum efficiency η. The first and second terms in Eq. (23) are due to informational and phase backactions, respectively. Note that the quantum regression formula [39] applied to the qubit state gives only the first term [30] and cannot be used in the case with phase backaction. Though theoretically $K(\tau)$ can exceed unity for any nonzero values of Ω_R and φ_a, in the experiment we need sufficiently fast Rabi oscillations and rather large φ_a to overcome experimental fluctuations. From Eq. (23) for $|\Omega_R| \gg \Gamma$, the maximum value of $K(\tau)$ is $K_{\rm max} \approx \sqrt{1 + c^2\tan^2\varphi_a}$.

The measurement setup is shown in Fig. 1 and further discussed in the Supplemental Material [38]. In the experiment we use $\Gamma = 1/1.8\ \mu$s, $\Omega_R/2\pi = \pm 1$ MHz, and $\varphi_a = 70°$. (In the Supplemental Material [38], we also present data for $\varphi_a = 0$, 40°, and 80°.) The averaged correlator (22) is obtained from the recorded data using $T = 0.28\ \mu$s and $t_{\rm skip} = 0.28\ \mu$s, so that $c = 0.79$ in Eq. (23). Figure 3(a) shows the experimental correlators $K_\pm(\tau)$, where the subscript indicates the sign of the product $x_0\Omega_R$ [38]. In each case the ensemble averaging is over 6.5×10^5 recorded traces. We see a good agreement between experiment (symbols) and theory (lines) in

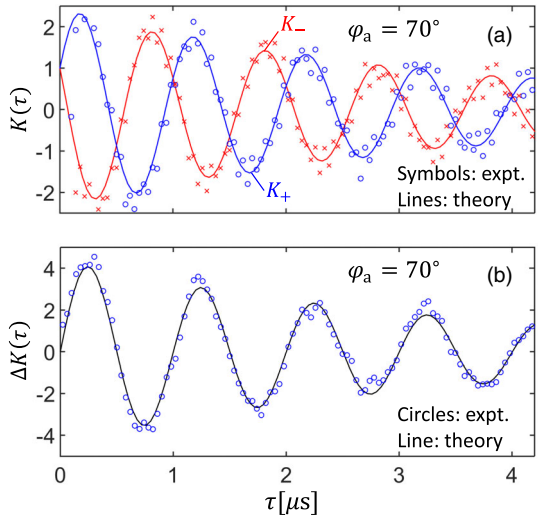

FIG. 3. Experimental correlators exceeding unity, for the phase misalignment $\varphi_a = 70°$, initial state $x_0 = \pm 1$, Rabi frequency $\Omega_R/2\pi = \pm 1$ MHz, and ensemble dephasing rate $\Gamma = 1/1.8\ \mu$s. Panel (a) shows the correlators $K_\pm$, with $\pm$ indicating the sign of $x_0\Omega_R$. Panel (b) shows the correlator difference $\Delta K(\tau) = K_+(\tau) - K_-(\tau)$. Experimental results are represented by symbols, the theory is shown by lines.

Fig. 3(a). Most importantly, experimental correlators reach values up to $K \simeq 2$, thus confirming that correlators can be larger than 1.

Figure 3(b) shows the correlator difference $\Delta K(\tau) \equiv K_+(\tau) - K_-(\tau)$. This difference is more immune to offset fluctuations of the detector outputs, so the experimental $\Delta K(\tau)$ is less noisy than $K_\pm(\tau)$ in Fig. 3(a). The experimental result (circles) in Fig. 3(b) agrees very well with the theoretical result (solid line) $\Delta K(\tau) = \tan\varphi_a \times 2c(\Omega_R/\tilde{\Omega}_R)\sin(\tilde{\Omega}_R\tau)e^{-\Gamma\tau/2}$.

The correlator difference $\Delta K(\tau)$ can be useful to accurately set $\varphi_a = 0$ in experiments that need to avoid phase backaction. At present this is typically done by maximizing the response $\Delta I(\varphi_a)$, which is not a sensitive calibration method due to the quadratic dependence of ΔI on φ_a near the maximum at $\varphi_a = 0$. In contrast, $\Delta K(\tau) \propto \tan\varphi_a$ vanishes at $\varphi_a = 0$ and depends linearly on φ_a in the vicinity (this still holds for the unscaled correlators), thus potentially providing a much better calibration accuracy (zero crossing detection is easy and accurate experimentally). The practical use of $\Delta K(\tau)$ for this purpose needs further investigation.

Note that the GCR provides an intuitive, but bizarre explanation for the correlators larger than 1. The same conclusion can be reached from the quantum Bayesian formalism but it lacks simplicity. In such formalism, the signal from the detector at time t_1 provides us some information about the fluctuating number of photons in the cavity, which moves the qubit along the equator of the Bloch sphere, thus affecting the z component of the qubit state at the later time t_2 due to Rabi rotations.

The GCR for multitime correlators.—In the case of simultaneous CQM of N_d noncommuting qubit observables $\sigma_\ell \equiv \boldsymbol{n}_\ell\boldsymbol{\sigma}$ (here $\boldsymbol{\sigma}$ is the vector of Pauli matrices, $\boldsymbol{n}_\ell$ is the ℓth measurement axis direction on the Bloch sphere, and $\ell = 1, 2, \ldots, N_d$), the GCR for an N-time correlator of the output signals $I_\ell(t)$ can be naturally generalized as [cf. Eq. (7)]

$$K_{\ell_1\ldots\ell_N}(t_1,\ldots t_N) \equiv \langle I_{\ell_N}(t_N)\cdots I_{\ell_2}(t_2)I_{\ell_1}(t_1)\rangle = \sum_{\{I_{\ell_j}=\pm1\}}^{2^N}\left[\prod_{j=2}^{j=N} I_{\ell_j}p(I_{\ell_j},t_j|I_{\ell_{j-1}},t_{j-1})\right] \times I_{\ell_1}p(I_{\ell_1},t_1), \quad (24)$$

where the time arguments are ordered as $t_1 < t_2 < \cdots < t_N$, $p(I_{\ell_1}, t_1)$ is given by Eq. (8) with $\boldsymbol{z}$ replaced by $\boldsymbol{n}_{\ell_1}$, and the conditional probability factors are

$$p(I_{\ell_j},t_j|I_{\ell_{j'}},t_{j'}) = \frac{1 + I_{\ell_j}\boldsymbol{n}_{\ell_j}\boldsymbol{r}_{\rm ens}(t_j|I_{\ell_{j'}}\boldsymbol{r}_{\rm coll}^{(j')},t_{j'})}{2}. \quad (25)$$

The collapsed state at time t_j is $I_{\ell_j}\boldsymbol{r}_{\rm coll}^{(j)}$, where

$$\boldsymbol{r}_{\rm coll}^{(j)} = \boldsymbol{n}_{\ell_j} + \mathcal{K}_{\ell_j}\boldsymbol{n}_{\ell_j}\times\boldsymbol{r}_{\rm ens}(t_j|I_{\ell_{j-1}}\boldsymbol{r}_{\rm coll}^{(j-1)},t_{j-1}) \quad (26)$$

for $j \geq 2$ [cf. Eq. (6)] and $\boldsymbol{r}_{\rm coll}^{(1)}$ is given by Eq. (6) with $\boldsymbol{z}$ and $\mathcal{K}$ replaced by $\boldsymbol{n}_{\ell_1}$ and $\mathcal{K}_{\ell_1}$, respectively. Parameters $\mathcal{K}_\ell = \tan\varphi_\ell^a$ characterize the relative strength of phase backaction in the ℓth detector [15]. In Eqs. (25)–(26), $\boldsymbol{r}_{\rm ens}$ obeys the evolution Eq. (5), where $\Lambda_{\rm ens}$ accounts for measurement of all σ_ℓ. This method to calculate N-time correlators is proven in the Supplemental Material [38]. Multitime and/or multidetector correlators can also exceed unity in the presence of phase backaction (with coherent evolution not always needed) [38].

Conclusions.—We have developed a recipe for the calculation of correlators in continuous qubit measurements with phase backaction. As a consequence of the effective evolution outside the Bloch sphere, the normalized correlators can exceed 1. This has been confirmed experimentally, with the correlator reaching the value of 2. The correlators can be used as a calibration tool.

The work was supported by ARO Grants No. W911NF-15-1-0496 and No. W911NF-18-10178.

*Present address: University of California, Berkeley, CA 94720, USA.
†Present address: Google Inc., Venice, CA 90291, USA.

[1] K. Kraus, A. Böhm, J. D. Dollard, and W. H. Wootters, *States, Effects, and Operations Fundamental Notions of Quantum Theory* (Springer, Berlin 1983).
[2] L. Diósi, Phys. Lett. A **129**, 419 (1988).
[3] J. Dalibard and Y. Castin, and K. Mølmer, Phys. Rev. Lett. **68**, 580 (1992).
[4] V. P. Belavkin, J. Multivariate Anal. **42**, 171 (1992).
[5] H. J. Carmichael, *An Open Systems Approach to Quantum Optics* (Springer, Berlin, 1993).
[6] H. M. Wiseman and G. J. Milburn, Phys. Rev. A **47**, 642 (1993).
[7] A. N. Korotkov, Phys. Rev. B **60**, 5737 (1999).
[8] J. Gambetta, A. Blais, M. Boissonneault, A. A. Houck, D. I. Schuster, and S. M. Girvin, Phys. Rev. A **77**, 012112 (2008).
[9] A. N. Korotkov, arXiv:1111.4016.
[10] N. Katz, M. Ansmann, R. C. Bialczak, E. Lucero, R. McDermott, M. Neeley, M. Steffen, E. M. Weig, A. N. Cleland, J. M. Martinis, and A. N. Korotkov, Science **312**, 1498 (2006).
[11] A. Palacios-Laloy, F. Mallet, F. Nguyen, P. Bertet, D. Vion, D. Esteve, and A. N. Korotkov, Nat. Phys. **6**, 442 (2010).
[12] M. Hatridge, S. Shankar, M. Mirrahimi, F. Schackert, K. Geerlings, T. Brecht, K. M. Sliwa, B. Abdo, L. Frunzio, S. M. Girvin, R. J. Schoelkopf, and M. H. Devoret, Science **339**, 178 (2013).
[13] K. W. Murch, S. J. Weber, C. Macklin, and I. Siddiqi, Nature (London) **502**, 211 (2013).
[14] D. Ristè, M. Dukalski, C. A. Watson, G. de Lange, M. J. Tiggelman, Ya. M. Blanter, K. W. Lehnert, R. N. Schouten, and L. DiCarlo, Nature (London) **502**, 350 (2013).

[15] S. Hacohen-Gourgy, L. S. Martin, E. Flurin, V. V. Ramasesh, K. B. Whaley, and I. Siddiqi, Nature (London) **538**, 491 (2016).
[16] Q. Ficheux, S. Jezouin, Z. Leghtas, and B. Huard, Nat. Commun. **9**, 1926 (2018).
[17] H. M. Wiseman and G. J. Milburn, Phys. Rev. Lett. **70**, 548 (1993).
[18] R. Ruskov and A. N. Korotkov, Phys. Rev. B **66**, 041401(R) (2002).
[19] R. Vijay, C. Macklin, D. H. Slichter, S. J. Weber, K. W. Murch, R. Naik, A. N. Korotkov, and I. Siddiqi, Nature (London) **490**, 77 (2012).
[20] G. de Lange, D. Ristè, M. J. Tiggelman, C. Eichler, L. Tornberg, G. Johansson, A. Wallraff, R. N. Schouten, and L. DiCarlo, Phys. Rev. Lett. **112**, 080501 (2014).
[21] T. L. Patti, A. Chantasri, L. P. García-Pintos, A. N. Jordan, and J. Dressel, Phys. Rev. A **96**, 022311 (2017).
[22] K. Jacobs, Phys. Rev. A **67**, 030301(R) (2003).
[23] R. Ruskov and A. N. Korotkov, Phys. Rev. B **67**, 241305(R) (2003).
[24] N. Roch, M. E. Schwartz, F. Motzoi, C. Macklin, R. Vijay, A. W. Eddins, A. N. Korotkov, K. B. Whaley, M. Sarovar, and I. Siddiqi, Phys. Rev. Lett. **112**, 170501 (2014).
[25] C. Ahn, A. C. Doherty, and A. J. Landahl, Phys. Rev. A **65**, 042301 (2002).
[26] H. Mabuchi, New J. Phys. **11**, 105044 (2009).
[27] R. Ruskov, A. N. Korotkov, and K. Mølmer, Phys. Rev. Lett. **105**, 100506 (2010).
[28] N. Foroozani, M. Naghiloo, D. Tan, K. Mølmer, and K. W. Murch, Phys. Rev. Lett. **116**, 110401 (2016).
[29] L. Diósi, Phys. Rev. A **94**, 010103(R) (2016).
[30] J. Atalaya, S. Hacohen-Gourgy, L. S. Martin, I. Siddiqi, and A. N. Korotkov, npj Quantum Inf. **4**, 41 (2018).
[31] A. Chantasri, J. Atalaya, S. Hacohen-Gourgy, L. S. Martin, I. Siddiqi, and A. N. Jordan, Phys. Rev. A **97**, 012118 (2018).
[32] J. Atalaya, S. Hacohen-Gourgy, L. S. Martin, I. Siddiqi, and A. N. Korotkov, Phys. Rev. A **97**, 020104(R) (2018).
[33] A. Tilloy, Phys. Rev. A **98**, 010104(R) (2018).
[34] J. Atalaya, M. Bahrami, L. P. Pryadko, and A. N. Korotkov, Phys. Rev. A **95**, 032317 (2017).
[35] A. N. Korotkov, Phys. Rev. A **94**, 042326 (2016).
[36] A. N. Korotkov, Phys. Rev. B **63**, 115403 (2001).
[37] Y. A. Aharonov, D. Z. Albert, and L. Vaidman, Phys. Rev. Lett. **60**, 1351 (1988).
[38] See Supplemental Material at http://link.aps.org/supplemental/10.1103/PhysRevLett.122.223603 for experimental details and proof of the GCR for multitime correlators in a multidetector case.
[39] C. W. Gardiner and P. Zoller, *Quantum Noise*, 3rd ed. (Springer, Berlin, 2004).